Title:
Collateral development and arteriogenesis in hindlimbs of domestic swine after ligation of arterial inflow

Author List:
Gao Y[#1], Patel NS[#1,2], , Aravind S[#1,2], Fuglestad M[1], Casale GP[1], *Pipinos II[##1,2], *Carlson MA[##1,2,3]

1. Department of Surgery, University of Nebraska Medical Center, Omaha, Nebraska
2. Surgery Department, Nebraska-Western Iowa Health Care System, Omaha, NE
3. Department of Genetics, Cell Biology and Anatomy, University of Nebraska Medical Center, Omaha, Nebraska

#These authors contributed equally
##These authors contributed equally

*Corresponding authors:
Iraklis I. Pipinos, MD (ipipinos@unmc.edu)
Mark A. Carlson, MD (macarlso@unmc.edu)

Department of Surgery
983280 Nebraska Medical Center
Omaha, NE 68198-3280
Tel.: 402-559-9549 (IIP); 402-995-5371 (MAC)
Fax: 402-559-6749

Emails:
Gao, Yue (ryan.gao@unmc.edu); Patel, Neesha S. (Neesha.patel@unmc.edu); Aravind, Shruthi (shruthi.aravind@unmc.edu); Fuglestad, Matthew (matthew.fuglestad@unmc.edu); Casale, George (gpcasale@unmc.edu); Pipinos, Iraklis I. (ipipinos@unmc.edu); Carlson, Mark A. (macarlso@unmc.edu)

Keywords: swine, porcine, animal models, arteriogenesis, ischemia, angiography, peripheral artery disease

ABSTRACT

Introduction. The development of collateral vasculature is a key mechanism compensating for arterial occlusions in patients with peripheral artery disease (PAD). We aimed to examine the development of collateral pathways after ligation of native vessels in a porcine model of PAD.

Methods: Right hindlimb Ischemia was induced in domestic swine (N=11, male, kg) using two different versions of arterial ligation. Version 1 (N=6) consisted of ligation/division of the right external iliac, profunda femoral and superficial femoral arteries. Version 2 (N=5) consisted of the ligation of Version 1 with additional ligation/division of the right internal iliac artery. Development of collateral pathways was evaluated with standard angiography at baseline (prior to arterial ligation) and at termination (4 weeks later). Relative luminal diameter of the arteries supplying the ischemic right hindlimb were determined by 2D angiography.

Results: The dominant collateral pathway that developed after Version 1 ligation connected the right internal iliac artery to the right profunda femoral and then to the right superficial femoral/popliteal artery. Mean luminal diameter of the right internal iliac artery at termination increased by 38% compared to baseline. Two co-dominant collateral pathways developed in Version 2 ligation: (i) from the left internal iliac artery to the reconstituted right internal iliac artery, which then supplied the right profunda femoral and then to the right superficial femoral/popliteal artery; and (ii) from the left profunda femoral artery to the reconstituted right profunda femoral artery. Mean diameter of the left internal iliac artery and left profunda artery increased at termination by 21% and 26%, respectively ($p < 0.05$).

Conclusion: Two versions of hindlimb ischemia induction (right ilio-femoral artery ligation with and without right internal iliac artery ligation) in swine produced differing collateral pathways,

along with changes to the diameter of the inflow vessels (i.e., arteriogenesis). Radiographic and anatomical data of the collateral formation in this porcine model should have value in investigation of the pathophysiology of hindlimb ischemia, and assessment of angiogenic therapies as potential treatments for PAD.

Abbreviations

AAALAC - Association for Assessment and Accreditation of Laboratory Animal Care International
ABI – Ankle/Brachial Index
CLI – Chronic Limb Ischemia
CIIT – Common Internal Iliac Trunk
DICOM - Digital Imaging and Communications in Medicine
dRPFA - reconstituted distal Right Profunda Femoral Artery
dRIIA - reconstituted distal Right Internal Iliac Artery
IACUC - Institutional Animal Care and Use Committee
LEIA – Left External Iliac Artery
LIIA – Left Internal Iliac Artery
LPFA – Left Profunda Femoral Artery
REIA – Right External Iliac Artery
RIIA – Right Internal Iliac Artery
RPFA – Right Profunda Femoral Artery
RSFA – Right Superficial Femoral Artery
RPop – Right Popliteal Artery
PAD – Peripheral Arterial Disease
Moxy – Muscle Oximetry
StO_2 – Muscle oxygen saturation
THb – Total Hemoglobin

INTRODUCTION

Peripheral artery disease (PAD) has a prevalence of 3-10% in the general population, with an impact on functional status, quality of life, and life expectancy [*1-3*]. The vast majority of symptomatic PAD patients present with exercise-associated leg discomfort and ambulatory disability known as intermittent claudication [*1-3*]; only 1-2% of patients present with critical ischemia, including severe pain at rest and/or tissue loss/gangrene. Treatment options for symptomatic PAD includes open and percutaneous revascularization but, after referral, only 13% of patients with claudication and 50% of patients with critical limb ischemia undergo a revascularization procedure [*4,5*]. These interventions rates are decreased by the presence of complex occlusive disease and/or medical comorbidities, both of which can limit walking ability and/or increase operative risk. For patients not undergoing revascularization, development of collateral blood flow is an important compensatory mechanism to improve blood flow to the ischemic limb, which makes the study of blood vessel growth in response to ischemia an important field of investigation.

The groups of Drs. Brewster and Lefer [*6,7*], in collaboration with our group, have demonstrated that two swine strains (with and without comorbidities) can recapitulate the pathophysiology of human PAD, including (i) persistently decreased hindlimb hemodynamics/perfusion, (ii) decreased treadmill performance, (iii) and ischemic myopathy (end-organ damage). The ability of swine to model human PAD prompted us to use a porcine model of PAD to determine: 1) the pathways and size of the collaterals developing over thirty days after two different versions of arterial ligation in the right hindlimb; and 2) the effect of these ligations and resulting collateral development on limb hemodynamics and oxygenation. The rationale for studying this collateralization phenomenon was to develop a clinically-relevant large-animal platform in which we could test the efficacy of cell-based therapies (or other interventions) in improving perfusion of the ischemic limb.

MATERIALS AND METHODS

Animal Welfare Statement. The animals utilized to generate the data for this report were maintained and treated in accordance with the *Guide for the Care and Use of Laboratory Animals* (8th ed.) from the National Research Council and the National Institutes of Health [*8*] and also in accordance with the Animal Welfare Act of the United States (U.S. Code 7, Sections 2131 – 2159). The animal protocol pertaining to this manuscript was approved by the Institutional Animal Care and Use Committee (IACUC) of the VA Nebraska-Western Iowa Health Care System (ID number 00950) and by the IACUC of the University of Nebraska Medical Center (ID number 15-068-07-ET). All procedures were performed in animal facilities approved by the Association for Assessment and Accreditation of Laboratory Animal Care International (AAALAC; www.aaalac.org) and by the Office of Laboratory Animal Welfare of the Public Health Service (grants.nih.gov/grants/olaw/olaw.htm). All surgical procedures were performed under isoflurane anesthesia, and all efforts were made to minimize suffering. Euthanasia was performed in accordance with the AVMA Guidelines for the Euthanasia of Animals [*9*].

Experimental Subjects. Wild type domestic swine (N = 13; castrated males; age 11-13 wk) were purchased from the Animal Research and Development Center at the University of Nebraska Lincoln (ardc.unl.edu). Swine were housed individually in pens, with multiple subjects per room, and fed ad lib with standard hog feed (Purina Nature's Match Sow and Pig Complete Feed).

Experimental Design. Refer to Fig. tf01. The basic experimental design included an ischemia-induction procedure (i.e., arterial ligation) on day 0, with endpoint measurement and necropsy

30 d later. Two methods of arterial ligation were compared in two nonrandomized groups of domestic swine; the groups were matched for age, size, and sex.

Set-Up and Anesthesia [*10*]. Swine were fasted for 24 h prior to the procedure, with free access to water and up to two 500 cc bottles of regular Gatorade™. On day zero, each subject underwent induction with ketamine (Zoetis, 2.2 mg/kg), Telazol® (Zoetis; 4.4 mg/kg) and xylazine (Zoetis; 2.2 mg/kg), given as a single IM injection. Each subject then was weighed and endotracheally intubated. EKG, pulse oximetry, rectal temperature, and lingual endtidal CO_2 monitors were placed. The subject rested on a water-circulated warming blanket that was set at 102˚F. An auricular intravenous (IV) line was placed. Anesthesia was maintained with isoflurane (0.5-1%) and supplemental oxygen (3-5 L/min) using a Matrx® ventilator (midmark.com). The ventilator rate initially was set at 12-15 breaths per minute with a tidal volume of 10 mL/kg, and subsequently adjusted to maintain the EtCO2 at 40-50 mm Hg. Cotton blankets were placed over non-surgical areas to minimize any decrease in body temperature. Vital signs were continuously recorded to a laptop computer via a Bionet BM5 monitor (www.bionetus.com). A single dose of cefovecin sodium (Zoetis; 8 mg/kg IM) was given before incision.

Muscle Oximetry & Arterial Indices. Extremity muscle oximetry measurements were measured transcutaneously in the supine position under general anesthesia using an ANT Fortiori Design device (Moxy device; moxymonitor.com) with Peripedal software (peripedal.com); see Figs. tf11S and tf12S. The Moxy device has a noninvasive probe which measures muscle hemoglobin/myoglobin oxygen saturation (StO_2). For determination of arterial indices, a pediatric-size sphygmomanometer cuff was applied to each extremity, about 10 cm above the hoof (see Fig. tf11S), and systolic pressure was measured with the aid of doppler device (Model 811-B, Parks Medical Doppler; parksmed.com). The hindlimb arterial pressure index (“ABI”, meant to be the porcine analog of the clinical ankle-brachial index) was defined as

the ratio of hindlimb systolic blood pressure over the higher of the two forelimb systolic pressures.

Laparotomy, Vessel Exposure, and Angiography. With the subject under general anesthesia and in the supine position, the chest, abdomen, groins, and bilateral lower extremities were shaved with an electric clipper, washed with soap and water, and then prepped using ChloraPrep™ applicators (chlorhexidine gluconate/isopropyl alcohol; BD Medical). Vessel exposure was obtained using a retroperitoneal approach through a right paramedian incision that just inferior to the urethral meatus and medial to the right nipple line, and then extended inferiorly across the right inguinal ligament (not divided) and onto the right inner thigh (Fig. tf10S), The abdominal wall layers were incised carefully down to the peritoneum, and then the dissection was performed laterally between the peritoneum and abdominal wall to develop the retroperitoneal space. The peritoneal sac, containing the intraabdominal organs, was retracted superiorly and to the left, which exposed the distal aorta and right-sided pelvic vasculature. In all subjects an arterial line (20-gauge Angiocatheter) was placed in the infrarenal aorta, 4-5 cm above the aortic trifurcation, through a site controlled with a 6-0 polypropylene U-stitch (see Fig. tf05, and the postmortem dissection in Fig. tf09S). This line was used for arterial blood pressure monitoring and angiography. A baseline aortogram with runoff was obtained with injection of 10 mL of Visipaque™ 320 (Iodixanol; GE Healthcare) and C-arm fluoroscopy (GE OEC 9900 Elite).

Arterial Interruption. Refer to Figs. tf05, tf02, and tf09S. Once baseline angiography was obtained, the region of the aortic trifurcation was dissected. In the pig, the distal aorta trifurcates into the right and left external iliac arteries (REIA and LEIA) and the common internal iliac trunk (CIIT); the latter then bifurcates into the right and left internal iliac arteries (RIIA and LIIA). The REIA was dissected down to the bifurcation of the right superficial femoral artery (RSFA) and profunda femoris artery (RPFA). The REIA, right lateral circumflex iliac and lateral circumflex

femoral artery (RLCIA and RLCFA, respectively) were suture ligated proximally with 3-0 silk. Distal dissection exposed the bifurcation of the RSFA into the right popliteal and saphena arteries (RPop and RSA). The RSFA was suture ligated distal to the takeoff of the RLCFA. A continuous segment of the REIA-RSFA was then excised (Figs. tf05 and tf02). This series of steps constituted the Version 1 arterial interruption procedure. Version 2 consisted of Version 1 plus ligation of the RIIA. To summarize:

Version 1 Interruption (Fig tf02B): ligation of the REIA, RSFA, RPFA, RLCIA, RLCFA and excision of a continuous segment of the REIA-RSFA.

Version 2 Interruption (Fig. tf02C): Version 1 + RIIA ligation

A completion angiogram was performed after arterial interruption was accomplished. The aortic puncture site utilized for angiographic access then was closed by tying the previously-placed U-stitch. The abdominal incision was closed anatomically in layers, with 2-0 polyglactin 910 in the peritoneum and posterior layers, 0-polydioxanone in the anterior aponeurosis, 3-0 polyglactin 910 in the panniculus carnosus, and 4-0 polyglactin 910 in the skin. Cyanoacrylate glue was applied over the skin incision; no other incisional dressing was applied. The animal's recovery from anesthesia was monitored until the subject was awake and mobile. Subjects were given half of their typical feed intake on post-ligation day 1, and were placed back on ad lib feeds on day 2.

Terminal procedure: Subjects underwent their terminal procedure 4 weeks after arterial interruption. After induction of general endotracheal anesthesia, the right carotid artery was exposed with a cervical cut-down. Hindlimb perfusion measurements (muscle oximetry and arterial indices) were performed as described above. A catheter was then placed into the right

common carotid artery and advanced into the aorta using the Seldinger technique. An abdominal aortogram with distal runoff was performed. Bilateral hindlimb dissection was performed prior to euthanasia. Biopsies of the medial heads of the bilateral gastrocnemius and plantaris muscles were harvested prior to euthanasia (Fig. tf13S) and processed as described under “Bright-Field Microscopy”.

Arterial Diameter Analysis: Each angiogram obtained during the procedure was saved into the Digital Imaging and Communications in Medicine (DICOM®) format within the GE OEC 9900 Elite C-arm instrument. Images subsequently were accessed and analyzed using the RadiANT DICOM Viewer (Version 4.0.2; www.radiantviewer.com). The cross-sectional diameter of the distal aorta was defined as 10 units. Relative diameter of each distal artery was then expressed in units of distal aortic diameter.

Bright-Field Microscopy: Porcine muscle specimens were fixed immediately in cold methacarn fixative for 48 h, transferred into cold 50% ethanol, and then embedded in paraffin. Sections (4 μm) from these blocks were deparaffinized in xylene, rehydrated in water, and then H&E stained. Bright field images were captured with a Leica DMRXA2 microscope configured with a Leica DFC color camera (North Central Instruments; www.ncimicro.com). Sections from archived paraffin blocks of human gastrocnemius muscle from deidentified patients (a claudicating PAD patient and a control subject) were similarly processed and imaged. These human specimens were obtained through an IRB protocol utilized for a separate study.

Statistical analysis: Data were analyzed using ANOVA within Microsoft Excel; the level of significance was defined as $p < 0.05$.

RESULTS

Perioperative Events. Mean starting weight in subjects who completed the study was 32.8 ± SD 4.0 kg (range = 26.6 – 39.0 kg, N = 6) and 37.0 ± 10.5 kg (range = 35.0 – 55.6 kg, N = 5) for Versions 1 and 2, respectively (p = 0.19, unpaired t-test). A total of 13 subjects underwent the ligation procedure. One pig developed non-reducible rectal prolapse four days after operation and was euthanized; another pig expired on postoperative day one secondary to intestinal ischemia. Necropsy of the latter subject revealed a stomach distended with feed and generalized severe ischemia (purplish discoloration) of the small and large intestine, but otherwise was inconclusive; specifically, all mesenteric vessels were patent. Of the eleven subjects which survived to the scheduled termination (N = 6 for Version 1 and N = 5 for Version 2), two subjects (one of each version) developed clinically-apparent ischemia of the right hoof, manifested by ulcer formation on the weight-bearing region. Their mobility was affected, but each animal could still ambulate and both survived until scheduled termination.

Arterial Pressure Indices at Rest. One subject's ABI data (Version 1) were missing, so ten subjects underwent analysis of ABI data. The ABI was calculated pre-ligation and immediately post-ligation on day 0, and then at pre-necropsy on day 30; see Table 1. The mean ABI was not different at rest between the two ligation versions at any individual time point, including at day 30. Immediately post-ligation, the ABI dropped to zero for both versions. At 30 d (pre-necropsy), the mean ABI had recovered in both groups to ~0.6.

Muscle hemoglobin/myoglobin oxygen saturation (StO_2) at Rest. StO_2 measurements were not different at rest between the two ligation versions at any single time point, including at day 30 (Fig. tf07). The StO_2 value decreased from 60-70% pre-ligation to ~20% immediately post-

ligation in both versions in the affected limb, with recovery to ~40% at 30 d (pre-necropsy). Interestingly, the contralateral (left, untreated) hindlimb demonstrated a parallel though less profound decrease in StO_2 after the right hindlimb interruption procedure, with partial recovery at 30 d (Fig. tf07).

Collateral Pathway Development. Refer to Videos 1-12 in the Supplemental Material. Sample images (video stills) of the pre-ligation (baseline) aortography with runoff for Versions 1 and 2 are shown in Figs. tf04A and tf06A, respectively (see accompanying Videos 1-2 and 7-8, respectively). Immediately after ligation in Version 1, the REIA-RSFA segment is no longer present and there is delayed filling of the RFPA and remaining distal arteries from the nonligated RIIA, with some minor contribution to the distal hindlimb through collaterals involving the RCIA (Fig. tf04B and Videos 3-4). After 30 days of ischemia in Version 1, pre-necropsy angiography (Fig. tf04C) demonstrated that the RIIA was noticeably enlarged, and that collateral vessels from the RIIA quickly reconstituted the RPFA, followed by the RSFA/RPop reconstitution (Video 5-6). There also appeared to be some minor contribution to RPFA/RSFA/RPop reconstitution via collaterals originating from lumbar vessels and involving the RCIA. Immediately after ligation in Version 2, both the REIA and RIIA are no longer visible. There is delayed filling of the RPFA from the LPFA via cross-pelvic collaterals, as shown in Fig. tf06B and Videos 9-10. In addition, there may have been some collateral supply to the ischemic hindlimb through collaterals originating from the right lumbar vessels immediately after ligation in Version 2 (Videos 9-10). After 30 days of ischemia in Version 2, pre-necropsy angiography (Fig. tf06C) demonstrated the presence of two co-dominant collateral pathways supplying the ischemic right hindlimb: (i) from the CIIT and LIIA to the reconstituted RIIA, subsequently supplying the RPFA and RSFA/RPop (Videos 11-12); and (ii) from the LPFA to the reconstituted RPFA (i.e., the same pathway noted immediately after ligation in Version 2).

Arteriogenesis. The relative arterial diameters of the hindlimb arteries at pre-ligation (day 0) and pre-necropsy (day 30) are shown in Table 2. Prior to ligation (i.e., day 0), the mean diameter of the LEIA and the dRPFA (distal right profunda femoral artery); were 6% and 30% larger, respectively, in the Version 2 compared to the Version 1 subjects ($p< 0.05$). The meaning of this difference in baseline arterial diameter between Version 1 vs. 2 subjects is not clear. After 30 days of ischemia in Version 1 subjects, the CIIT, RIIA, and dRPFA increased in diameter by 17%, 38%, and 17%, respectively ($p < 0.05$); the LIIA and RPop both trended toward increased diameter, but did not reach significance. The dRPFA and RPop both represented reconstituted vessels at 30 days. After 30 days of ischemia in Version 2 subjects, the CIIT, LEIA, LIIA, and LPFA all had a diameter increase in the range of 20% (23%, 18%, 21%, and 26%, respectively); the dRPFA trended toward increased diameter, but this did not reach significance. The only vessel noted to have a decrease in mean diameter at 30 days was the RPop in the Version 2 subjects, which decreased by 21%.

Ischemic Myopathy. Chronically ischemic muscle from both porcine and human subjects exhibited microscopic features of ischemic myopathy (Fig. tf08). H&E micrographs of chronically ischemic (day 30) vs. control (contralateral) porcine gastrocnemius muscle are shown in Fig. tf08A & C, respectively, along with analogous micrographs of gastrocnemius muscle from a claudicating PAD patient and a control non-PAD patient (Fig. tf08B & D, respectively). Control muscle from both swine (Fig. tf08A) and humans (Fig. tf08B) demonstrated polygonal myofibers having relatively similar shape and size, with barely perceptible endomysium and perimysium. However, in ischemic muscle from both swine (Fig. tf08C) and humans (Fig. tf08D), there was a wide range of myofiber size and shape, with thickening/fibrosis of the endomysium and perimysium. The myopathic features and other characteristics of chronically ischemic muscle from PAD patients has been previously described [*11-14*].

DISCUSSION

Herein we have described the pattern and relative size of the collateral pathways that develop after ligation of the native iliofemoral pedicle in a porcine model of PAD. These data demonstrate that two versions of hindlimb ischemia induction (right iliofemoral artery ligation/excision with and without right internal iliac artery ligation) produce differing collateral pathways along with outward remodeling/arteriogenesis (seen as increases of the diameter) of the major inflow vessels. We found that after ligation and excision of the right iliofemoral artery a dominant pathway developed which connected the patent RIIA to the reconstituted RPFA and RSFA/popliteal artery of the ischemic limb. However, after ligation and excision of the right iliofemoral artery with concomitant ligation of the RIIA, two co-dominant collateral pathways developed: (i) the first connected the common internal iliac trunk and left internal iliac artery to the reconstituted RIIA, which then supplied the reconstituted RPFA and RSFA/popliteal arteries: (ii) the second connected the left profunda artery to the reconstituted RPFA. Our data has confirmed previous findings from the groups of Drs. Brewster and Lefer [*6,7*].

Of note, three strains of swine have been tested to date as models of human PAD: (i) Ossabaw mini-swine fed a high-fat diet in order to mimic metabolic syndrome [*6*]; (ii) Yorkshire swine fed regular chow [*7*]; and (iii) and domestic swine fed regular chow (present report). It appears that all of these models, which have utilized both endovascular and open arterial interruption, have demonstrated the ability to recapitulate the pathophysiologic characteristics of human PAD, including decreased hindlimb hemodynamics/perfusion and ischemic myopathy (i.e., end-organ damage). The use of domestic swine fed regular chow along with an open arterial ligation technique allows for relative a cost saving (a less expensive animal and diet, and lower cost of operative and device supplies). In addition, the open ligation approach does not require specialized endovascular experience or operative setup, yet retains the ability to tailor the degree of ischemia.

The development of collateral vasculature is a key mechanism which compensates for arterial occlusion in PAD, and has the potential to be manipulated therapeutically to treat afflicted patients. In particular, the advent of different angiogenic therapies for humans, including administration of angiogenic cytokines (either as recombinant protein or with gene therapy) and, more recently, investigations of stem/progenitor cell therapy, has opened a new frontier in therapeutic opportunities for PAD [*15-17*]. We believe that the present report can serve as a reference for future studies on novel therapeutic interventions that would enhance collateral growth. For example, a porcine model could help in the optimization of delivery methods, dosing, efficacy testing of experimental arteriogenic treatments, including cell-based therapies [*16,18-21*].

A unique aspect of this project was the careful characterization of arteriogenesis and collateral formation. We were able to demonstrate specific locations within the porcine vascular network that experienced the greatest luminal growth after induction of ischemia. Quantification of arterial growth at specific sites was used to support the descriptive finding of reproducible collateral formation that were observed in both versions of hindlimb ischemia during angiography. Arteriogenesis is thought to be a reactive process to blood flow redistribution that occurs in occlusive disease [*22-25*]. Changes in fluid dynamics within patent arteries nearby an occlusion causes an increase in shear forces that leads to upregulation of cell adhesion molecules and nitric oxide production in endothelial cells, with a subsequent rise in cytokine and growth factor release, which leads to endothelial and smooth cell proliferation, and a persistent increase (i.e., structural change) in arterial lumen. Given the current understanding of the pathophysiology of the vessel remodeling that occurs in PAD, we can use the swine ischemia model for quantitative testing of arteriogenic therapies, as well as to investigate and improve delivery methods and dosing regimens.

Regarding the two premature mortalities in this study, rectal prolapse is common in growing swine from 8-20 weeks old [*26*]. The prolapse in our study may have been exacerbated

by increased intraabdominal pressure from postoperative ileus. The subject which died from intestinal ischemia had a stomach distended from recent feeding; this apparently was a consequence of noncompliance with the prescribed 24 h preoperative fast. This noncompliance (i.e., inappropriate access to feeds) appeared to be an isolated event, as other subjects did not have postoperative intraabdominal issues. The development of hoof ulcers in two of the surviving eleven subjects demonstrated that some subjects may have had critical limb ischemia.

Limitations of this study which could impact the validity of our porcine PAD model include its acute onset of ischemia, which differs from the more progressive and chronic nature of human PAD. Another limitation concerns mimicry of clinical conditions; while PAD patients often are aged and have comorbidities such as hypertension, dyslipidemia, and diabetes, our domestic swine were juvenile, without comorbidities. Regarding hemodynamic and perfusion measurements, all data were collected at rest under anesthesia, so relevant exercise-induced phenomena could have been missed. Regarding quantification of arteriogenesis, only larger inflow arteries were evaluated, so growth in smaller, unnamed collateral arteries may also have been missed. Future work can incorporate comorbidities into the model, and/or acquire measurements during stress maneuvers (e.g., post-occlusive hyperemia or exercise). In comparison to a porcine model utilizing endovascular occlusion [ref], the model described herein requires a large incision for the arterial ligations. The degree of tissue trauma and pain associated with this open procedure might be a confounding factor when studying functional status (e.g., gait, treadmill performance) of the subjects.

CONCLUSION

We documented collateral network formation and quantified arteriogenesis in our open model of porcine hindlimb ischemia model. These phenomena are important compensatory mechanisms in the ischemic lower extremity of the patient with symptomatic PAD. Using the

porcine model and the measurements described herein, we intend to develop, study, and optimize therapies for the treatment of PAD, particularly for patients whose revascularization options are limited.

REFERENCES

1. Criqui MH, Fronek A, Barrett-Connor E, Klauber MR, Gabriel S, Goodman D. The prevalence of peripheral arterial disease in a defined population. *Circulation*. 1985;71(3):510-515. PMID: 3156006. doi:
2. Hiatt WR, Hoag S, Hamman RF. Effect of diagnostic criteria on the prevalence of peripheral arterial disease. The San Luis Valley Diabetes Study. *Circulation*. 1995;91(5):1472-1479. PMID: 7867189. doi:
3. Selvin E, Erlinger TP. Prevalence of and risk factors for peripheral arterial disease in the United States: results from the National Health and Nutrition Examination Survey, 1999-2000. *Circulation*. 2004;110(6):738-743. PMID: 15262830. doi: 10.1161/01.CIR.0000137913.26087.F0
4. Devine EB, Alfonso-Cristancho R, Yanez ND, Edwards TC, Patrick DL, Armstrong CA*, et al.* Effectiveness of a Medical vs Revascularization Intervention for Intermittent Leg Claudication Based on Patient-Reported Outcomes. *JAMA Surg*. 2016;151(10):e162024. PMID: 27760274. doi: 10.1001/jamasurg.2016.2024
5. Norgren L, Hiatt WR, Dormandy JA, Nehler MR, Harris KA, Fowkes FG. Inter-Society Consensus for the Management of Peripheral Arterial Disease (TASC II). *J Vasc Surg*. 2007;45 Suppl S:S5-67. PMID: 17223489. doi: 10.1016/j.jvs.2006.12.037
6. Polhemus DJ, Bradley JM, Islam KN, Brewster LP, Calvert JW, Tao YX*, et al.* Therapeutic potential of sustained-release sodium nitrite for critical limb ischemia in the setting of metabolic syndrome. *Am J Physiol Heart Circ Physiol*. 2015;309(1):H82-92. PMID: 25910804. doi: 10.1152/ajpheart.00115.2015
7. Long CA, Timmins LH, Koutakis P, Goodchild TT, Lefer DJ, Pipinos, II*, et al.* An endovascular model of ischemic myopathy from peripheral arterial disease. *J Vasc Surg*. 2017;66(3):891-901. PMID: 27693032. doi: 10.1016/j.jvs.2016.07.127

8. Committee for the Update of the Guide for the Care and Use of Laboratory Animals. *Guide for the Care and Use of Laboratory Animals*: Washington, DC: The National Academies Press; 2011.

9. American Veterinary Medical Association Panel on Euthanasia. *AVMA Guidelines for the Euthanasia of Animals: 2013 Edition*. Schaumberg, IL: American Veterinary Medical Association; 2013.

10. Swindle MM, Smith AC. *Swine in the Laboratory: Surgery, Anesthesia, Imaging, and Experimental Techniques*. 3rd ed. Boca Raton, FL: CRC Press; 2016.

11. Pipinos, II, Swanson SA, Zhu Z, Nella AA, Weiss DJ, Gutti TL*, et al.* Chronically ischemic mouse skeletal muscle exhibits myopathy in association with mitochondrial dysfunction and oxidative damage. *Am J Physiol Regul Integr Comp Physiol*. 2008;295(1):R290-296. PMID: 18480238. doi: 10.1152/ajpregu.90374.2008

12. Cluff K, Miserlis D, Naganathan GK, Pipinos, II, Koutakis P, Samal A*, et al.* Morphometric analysis of gastrocnemius muscle biopsies from patients with peripheral arterial disease: objective grading of muscle degeneration. *Am J Physiol Regul Integr Comp Physiol*. 2013;305(3):R291-299. PMID: 23720135. doi: 10.1152/ajpregu.00525.2012

13. Papoutsi E CG, Koutakis P, Myers S, Thompson JR, Ha D, Swanson SA, Zhu Z, Kim K, Wurdeman S, Johanning JM, McComb RD, Pipinos II. Revascularization Improves the Myopathy, Hemodynamics and Function of the Limbs of Patients With Peripheral Arterial Disease *Circulation*. 2013;128:A19103. PMID: doi:

14. Weiss DJ, Casale GP, Koutakis P, Nella AA, Swanson SA, Zhu Z*, et al.* Oxidative damage and myofiber degeneration in the gastrocnemius of patients with peripheral arterial disease. *J Transl Med*. 2013;11:230. PMID: 24067235. doi: 10.1186/1479-5876-11-230

15. Cooke JP, Losordo DW. Modulating the vascular response to limb ischemia: angiogenic and cell therapies. *Circ Res*. 2015;116(9):1561-1578. PMID: 25908729. doi: 10.1161/CIRCRESAHA.115.303565

16. Frangogiannis NG. Cell therapy for peripheral artery disease. *Curr Opin Pharmacol*. 2018;39:27-34. PMID: 29452987. doi: 10.1016/j.coph.2018.01.005

17. Parikh PP, Liu ZJ, Velazquez OC. A Molecular and Clinical Review of Stem Cell Therapy in Critical Limb Ischemia. *Stem Cells Int*. 2017;2017:3750829. PMID: 29358955. doi: 10.1155/2017/3750829

18. Aranguren XL, Verfaillie CM, Luttun A. Emerging hurdles in stem cell therapy for peripheral vascular disease. *J Mol Med (Berl)*. 2009;87(1):3-16. PMID: 18712330. doi: 10.1007/s00109-008-0394-3

19. Gupta NK, Armstrong EJ, Parikh SA. The current state of stem cell therapy for peripheral artery disease. *Curr Cardiol Rep*. 2014;16(2):447. PMID: 24414120. doi: 10.1007/s11886-013-0447-2

20. Lawall H, Bramlage P, Amann B. Treatment of peripheral arterial disease using stem and progenitor cell therapy. *J Vasc Surg*. 2011;53(2):445-453. PMID: 21030198. doi: 10.1016/j.jvs.2010.08.060

21. Qadura M, Terenzi DC, Verma S, Al-Omran M, Hess DA. Concise Review: Cell Therapy for Critical Limb Ischemia: An Integrated Review of Preclinical and Clinical Studies. *Stem Cells*. 2018;36(2):161-171. PMID: 29226477. doi: 10.1002/stem.2751

22. Carmeliet P, Eelen G, Kalucka J. Arteriogenesis versus angiogenesis. In: Krams R, Bäck M, editors. *The ESC Textbook of Vascular Biology*: Oxford University Press; 2017.

23. Deindl E, Schaper W. The art of arteriogenesis. *Cell Biochem Biophys*. 2005;43(1):1-15. PMID: 16043879. doi: 10.1385/CBB:43:1:001

24. Rizzi A, Benagiano V, Ribatti D. Angiogenesis versus arteriogenesis. *Rom J Morphol Embryol*. 2017;58(1):15-19. PMID: 28523292. doi:

25. van Royen N, Piek JJ, Schaper W, Fulton WF. A critical review of clinical arteriogenesis research. *J Am Coll Cardiol*. 2009;55(1):17-25. PMID: 20117358. doi: 10.1016/j.jacc.2009.06.058

26. Garden S. Rectal prolapse in pigs. *Vet Rec*. 1988;123(25):654. PMID: 3218053. doi:

ACKNOWLEDGEMENTS

This work was supported by NIH grants R01 AG034995 and R01 AG049868, by the Charles and Mary Heider Fund for Excellence in Vascular Surgery, and by internal seed funds from the Department of Surgery of the University of Nebraska Medical Center. This work was supported with resources and the use of facilities at the VA Nebraska-Western Iowa Health Care System. Portions of this study were presented at Vascular Discovery: From Genes to Medicine (San Francisco, CA; May, 2018). The authors would like to acknowledge the technical assistance of Chris Hansen.

DISCLOSURES

The authors declare no competing interests.

FIGURE LEGENDS

Legends for Fig. tf01-tf08 are contained within the Figures.

SUPPLEMENTAL MATERIAL

Figures tf09S-tf13S.

Videos

1. “Vid01_v1_PreLigAngio_Proximal.mp4”. Description: Version 1 aortobifemoral angiography shot pre-ligation, proximal view.
2. “Vid02_v1_PreLigAngio_Distal.mp4”. Description: Version 1 aortobifemoral angiography shot pre-ligation, distal view.
3. “Vid03_v1_PostLigAngio_Proximal.mp4”. Description: Version 1 aortobifemoral angiography shot immediately post-ligation, proximal view.
4. “Vid04_v1_PostLigAngio_Distal.mp4”. Description: Version 1 aortobifemoral angiography shot immediately post-ligation, distal view.
5. “Vid05_v1_PreNecAngio_Proximal.mp4”. Description: Version 1 aortobifemoral angiography shot immediately pre-necropsy (30 days after ligation), proximal view.
6. “Vid06_v1_PreNecAngio_Distal.mp4”. Description: Version 1 aortobifemoral angiography shot immediately pre-necropsy (30 days after ligation), distal view.
7. “Vid07_v2_PreLigAngio_Proximal.mp4”. Description: Version 2 aortobifemoral angiography shot pre-ligation, proximal view.
8. “Vid08_v2_PreLigAngio_Distal.mp4”. Description: Version 2 aortobifemoral angiography shot pre-ligation, distal view.
9. “Vid09_v2_PostLigAngio_Proximal.mp4”. Description: Version 2 aortobifemoral angiography shot immediately post-ligation, proximal view.
10. “Vid10_v2_PostLigAngio_Distal.mp4”. Description: Version 2 aortobifemoral angiography shot immediately post-ligation, distal view.
11. “Vid11_v2_PreNecAngio_Proximal.mp4”. Description: Version 2 aortobifemoral angiography shot immediately pre-necropsy (30 days after ligation), proximal view.
12. “Vid12_v2_PreNecAngio_Distal.mp4”. Description: Version 2 aortobifemoral angiography shot immediately pre-necropsy (30 days after ligation), distal view.

Table 1. Arterial pressure indices ("ABI") of right (ischemic) hindlimb in Version 1 vs. 2.

	Day 0			
Version (N)	ABI, pre	ABI, post	ABI, Day 30	*ANOVA
1 (N = 5)	1.00 ± 0.22	0	0.62 ± 0.25	0.0001
2 (N = 5)	1.24 ± 0.30	0	0.62 ± 0.35	0.0004
*Unpaired t-test	0.196	1.000	0.968	

ABI expressed as mean ± standard deviation. Terms "pre" and "post" refer to before and after arterial ligation. The 30 d ABI was determined immediately prior to necropsy. *p-values.

Table 2. Relative hindlimb arterial diameters, Version 1 vs. 2, at days 0 vs. 30.

	CIIT		LEIA		RIIA		LIIA		dRPFA		LPFA		RPop	
VERSION 1	Day 0	Day 30	Day 0	Day 30	Day 0	Day 30	Day 0	Day 30	Day 0	†Day 30	Day 0	Day 30	Day 0	†Day 30
Mean	6.70	7.87	5.51	5.37	3.75	5.19	3.65	3.85	2.58	3.02	3.25	3.25	3.24	3.00
SD	0.34	0.44	0.27	0.26	0.31	0.22	0.19	0.24	0.29	0.25	0.25	0.39	0.37	0.32
*Paired t	**0.0049**		0.1901		**0.0001**		0.0702		**0.0228**		0.4936		0.0529	
	CIIT		LEIA		dRIIA		LIIA		dRPFA		LPFA		RPop	
VERSION 2	Day 0	Day 30	Day 0	Day 30	Day 0	†Day 30	Day 0	Day 30	Day 0	†Day 30	Day 0	Day 30	Day 0	†Day 30
Mean	6.68	8.24	5.84	6.92	3.13	3.44	3.90	4.72	3.35	3.67	3.50	4.42	3.37	2.65
SD	0.26	0.85	0.32	0.75	0.24	0.74	0.33	0.33	0.39	0.18	0.35	1.03	0.39	0.40
*Paired t	**0.0158**		**0.0133**		0.1304		**0.0044**		0.0591		**0.0207**		**0.0187**	
**Unpaired t	0.4678	0.1892	**0.0465**	**0.0005**	**NA**	**NA**	0.0727	**0.0004**	**0.0023**	**0.0004**	0.0917	**0.0145**	0.2892	0.0710

Relative diameter of each artery was expressed in units of distal aortic diameter (which was defined as 10 within each angiogram). Day 0 = pre-ligation measurement. Day 30 = pre-necropsy measurement. CIIT = common internal iliac trunk; LEIA = left external iliac artery; RIIA = right internal iliac artery; LIIA = left internal iliac artery; dRPFA = reconstituted distal right profunda femoral artery; LPFA = left profunda femoral artery; RPop = right popliteal artery; dRIIA = reconstituted distal right internal iliac artery. *Paired t-test compared day 0 vs. 30 for each artery (p-value). **Unpaired t-test compared Version 1 vs. Version 2 at each time point (p-value). †Reconstituted vessel. NA = comparison not applicable (RIIA was measured in Version 1, dRIIA was measured in Version 2).

Main figures

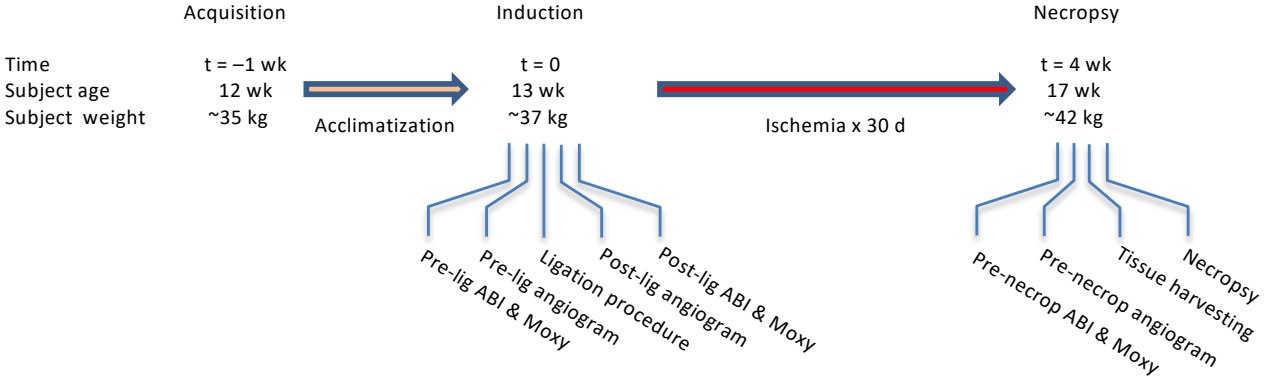

Fig. tf01. Experimental flow diagram. Domestic swine were 3 mo old at time of acquisition (t = -1 wk).

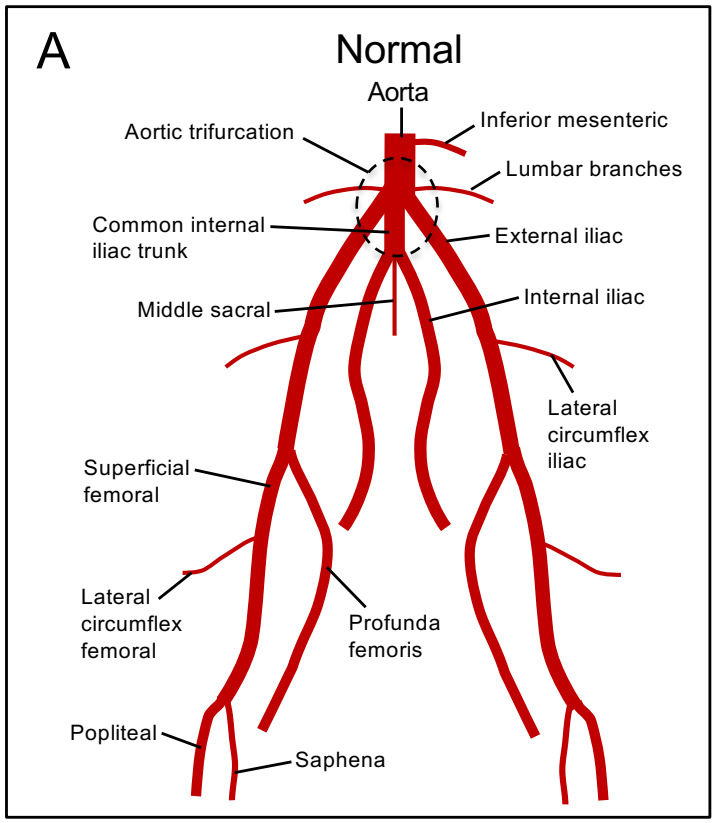

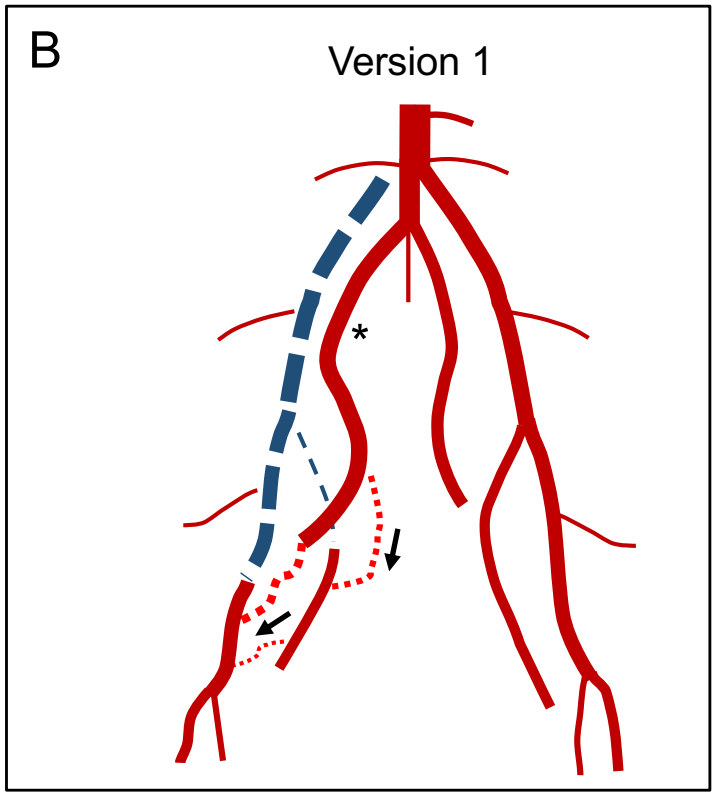

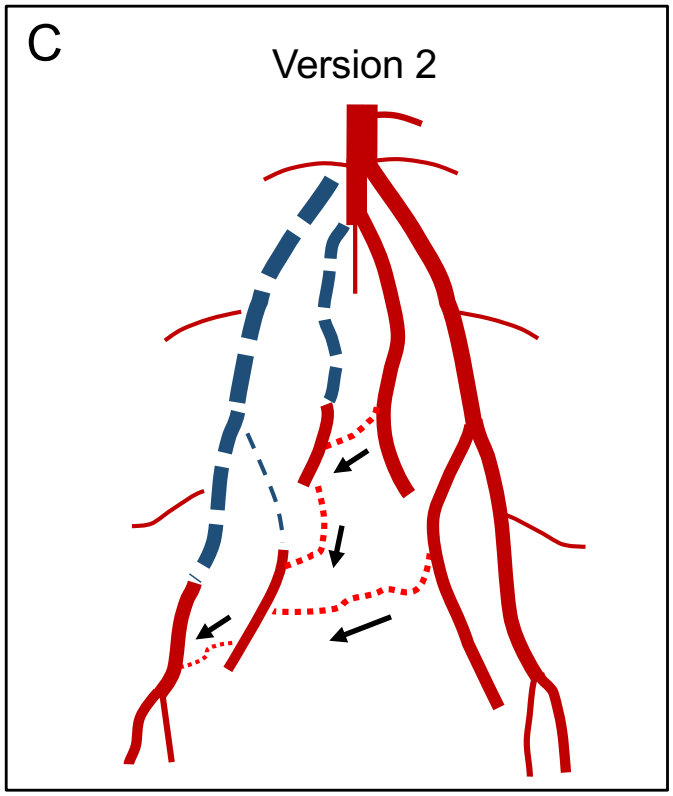

Fig. tf02. Arterial anatomy of the porcine hindlimb. **(A)** Normal anatomy. **(B)** Ligation Version 1. The right iliofemoral segment has been ligated and excised (thick dashed blue line), along with the right profunda femoris (thin dashed blue line). One month after ligation, the right internal iliac artery has enlarged (*), and there is collateral flow from this vessel which reconstitutes both the distal superficial femoral artery and the distal right profunda femoris (black arrows). **(C)** Ligation Version 2. In addition to the ligations performed for Version 1, the right internal iliac vessel has ligated. One month after ligation, collaterals from the left internal iliac artery reconstitute the right internal iliac, which then reconstitutes the right profunda femoris and distal superficial femoral artery through further collateralization (black arrows). The left profunda femoris helps reconstitute the right profunda femoris through separate collateralization.

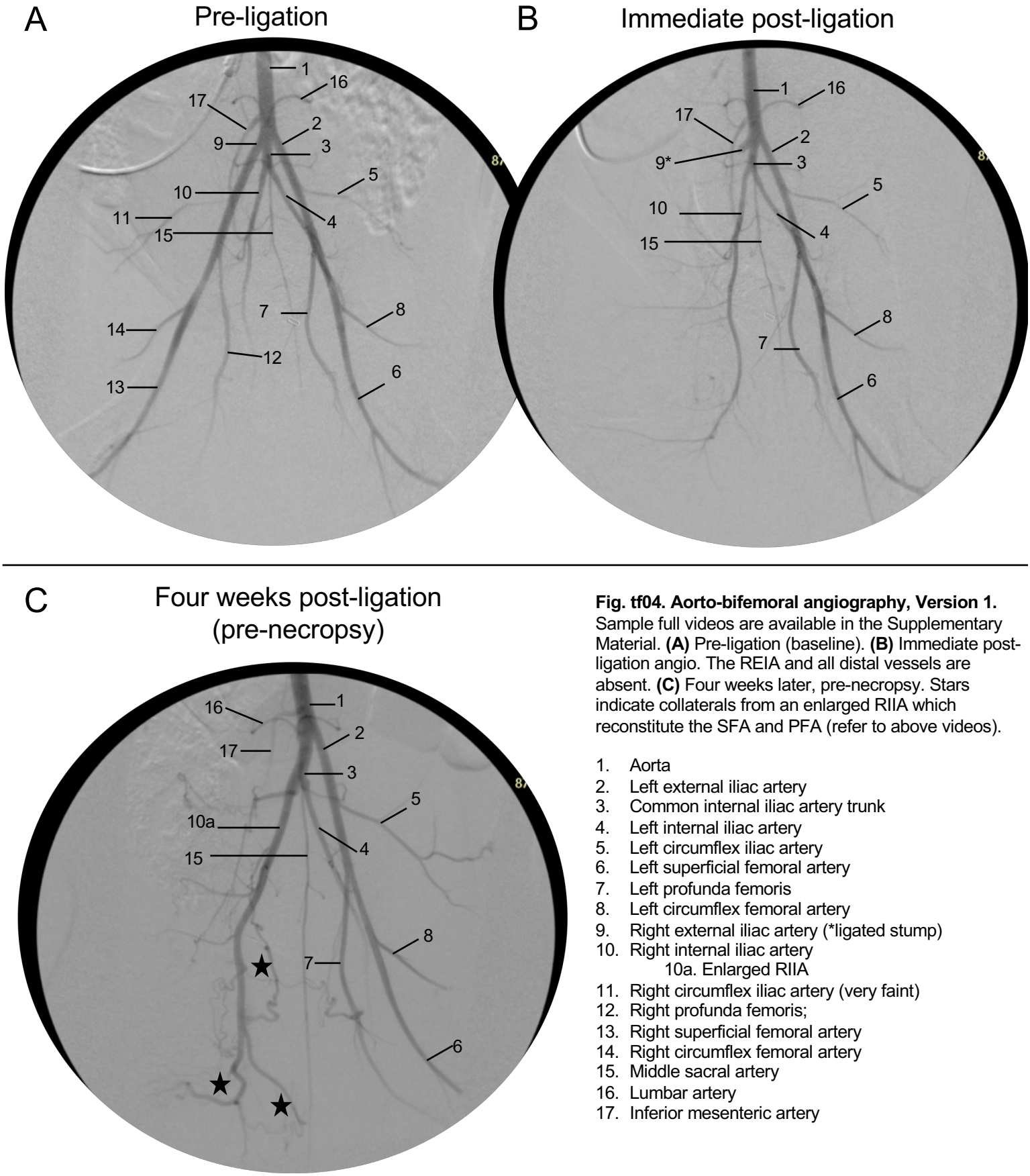

Fig. tf04. Aorto-bifemoral angiography, Version 1. Sample full videos are available in the Supplementary Material. **(A)** Pre-ligation (baseline). **(B)** Immediate post-ligation angio. The REIA and all distal vessels are absent. **(C)** Four weeks later, pre-necropsy. Stars indicate collaterals from an enlarged RIIA which reconstitute the SFA and PFA (refer to above videos).

1. Aorta
2. Left external iliac artery
3. Common internal iliac artery trunk
4. Left internal iliac artery
5. Left circumflex iliac artery
6. Left superficial femoral artery
7. Left profunda femoris
8. Left circumflex femoral artery
9. Right external iliac artery (*ligated stump)
10. Right internal iliac artery
    10a. Enlarged RIIA
11. Right circumflex iliac artery (very faint)
12. Right profunda femoris;
13. Right superficial femoral artery
14. Right circumflex femoral artery
15. Middle sacral artery
16. Lumbar artery
17. Inferior mesenteric artery

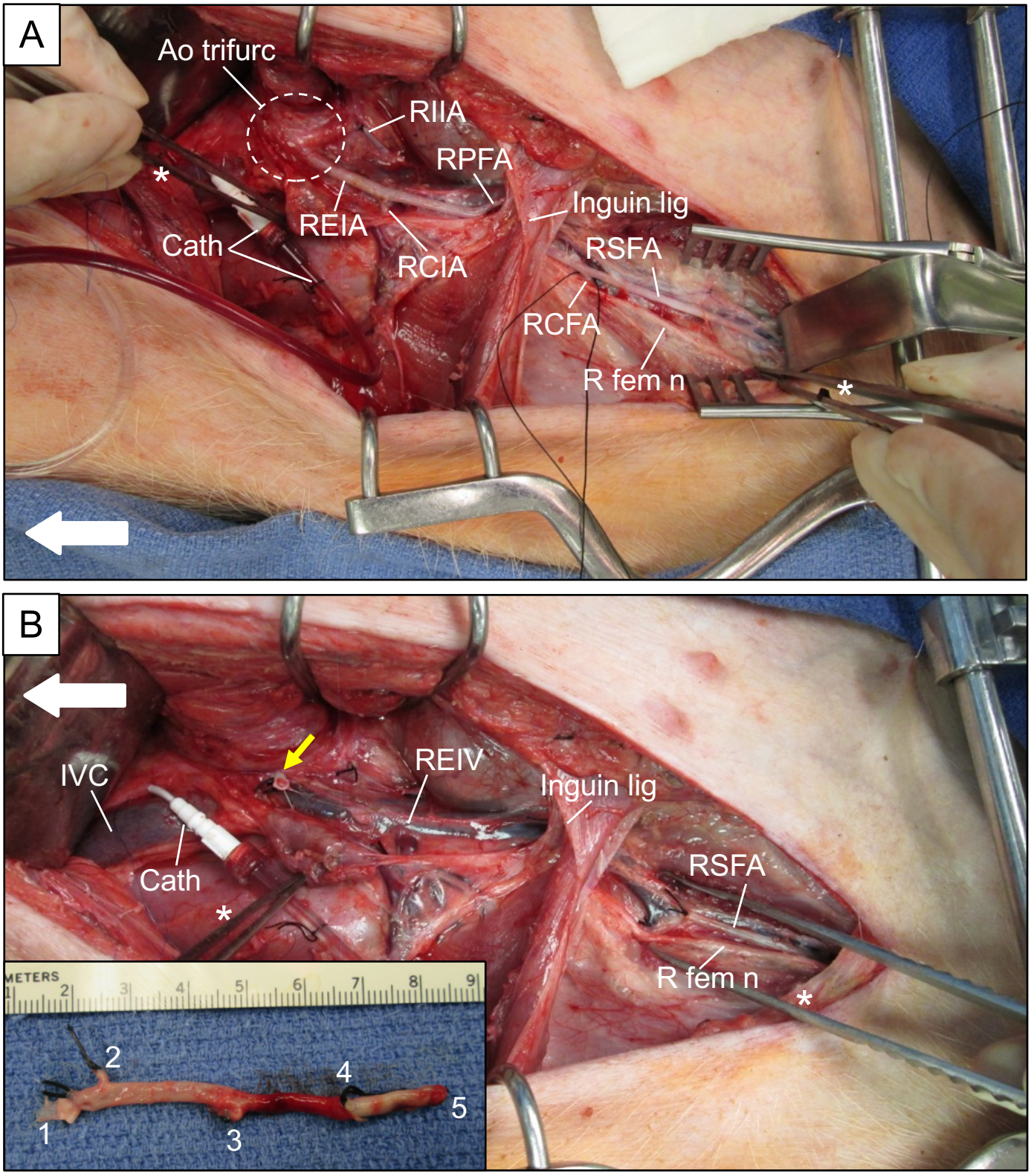

Fig. tf05. Ligation-excision procedure (Version 2), intraoperative photos. **(A)** Prior to ligation, showing a right retroperitoneal dissection. Large white arrow is superior. The viscera have been retracted medially and superiorly. The right iliofemoral complex has been dissected out above and below the inguinal ligament (Inguin lig). The region of the aortic trifurcation (Ao trifurc) is indicated with a dashed white circle. The right internal iliac artery (RIIA) already has been ligated (only for Version 2). There is a silk loop around the right circumflex femoral artery (RCFA). Cath = angiography cather & line; REIA = right external iliac artery; RCIA = right circumflex iliac artery; RPFA = right profunda femoris artery; RSFA = right superficial femoral artery; R fem n = right femoral nerve. **(B)** The right iliofemoral complex has been ligated and excised down to the distal RSFA, with ligation of the RPFA and RCIA. The right external iliac vein (REIV) is visible in the bed of the resected artery. The yellow arrow indicates the stump of the ligated REIA. DeBakey forceps indicated with asterisk (*). **Inset**: resected right iliofemoral complex. Vessel stumps: 1 = REIA; 2 = RCIA; 3 = RPFA; 4 = RCFA; 5 = RSFA.

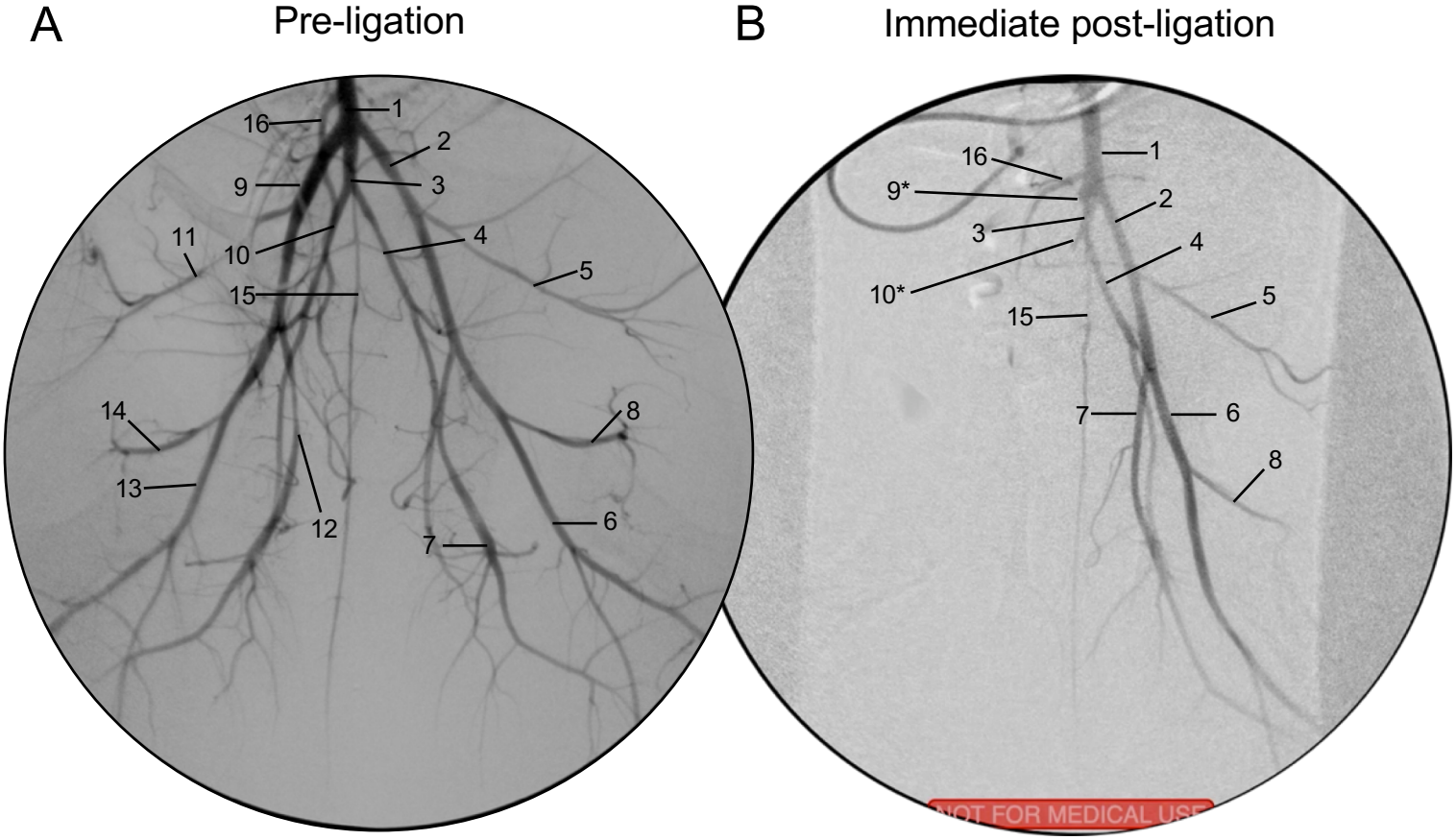

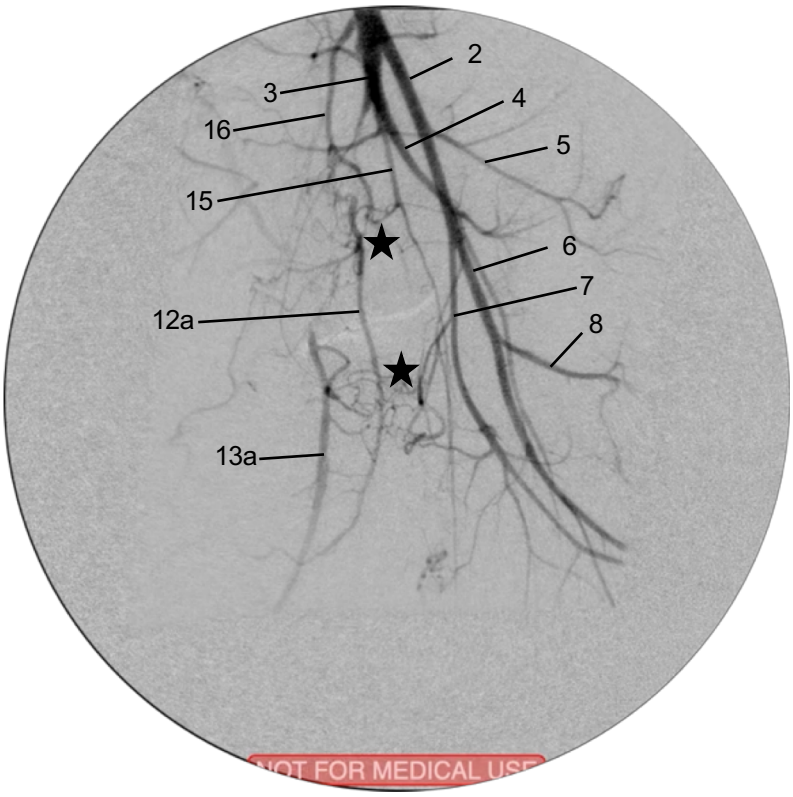

Fig. tf06. Aorto-bifemoral angiography, Version 2. Sample full videos are available in the Supplementary Material. **(A)** Pre-ligation (baseline). **(B)** Immediate post-ligation angio. The REIA, RIIA, and all distal vessels are absent. **(C)** Four weeks later, pre-necropsy. Stars indicate cross-over collaterals from LIIA and LPFA which reconstitute the RSFA and RPFA (refer to above videos).

1. Aorta
2. Left external iliac artery
3. Common internal iliac artery trunk
4. Left internal iliac artery
5. Left circumflex iliac artery
6. Left superficial femoral artery
7. Left profunda femoris
8. Left circumflex femoral artery
9. Right external iliac artery
10. Right internal iliac artery (*ligated stump)
11. Right circumflex iliac artery
12. Right profunda femoris
    - 12a. Reconstituted RPFA
13. Right superficial femoral artery
    - 13a. Reconstituted RSFA
14. Right circumflex femoral artery
15. Middle sacral artery
16. Inferior mesenteric artery

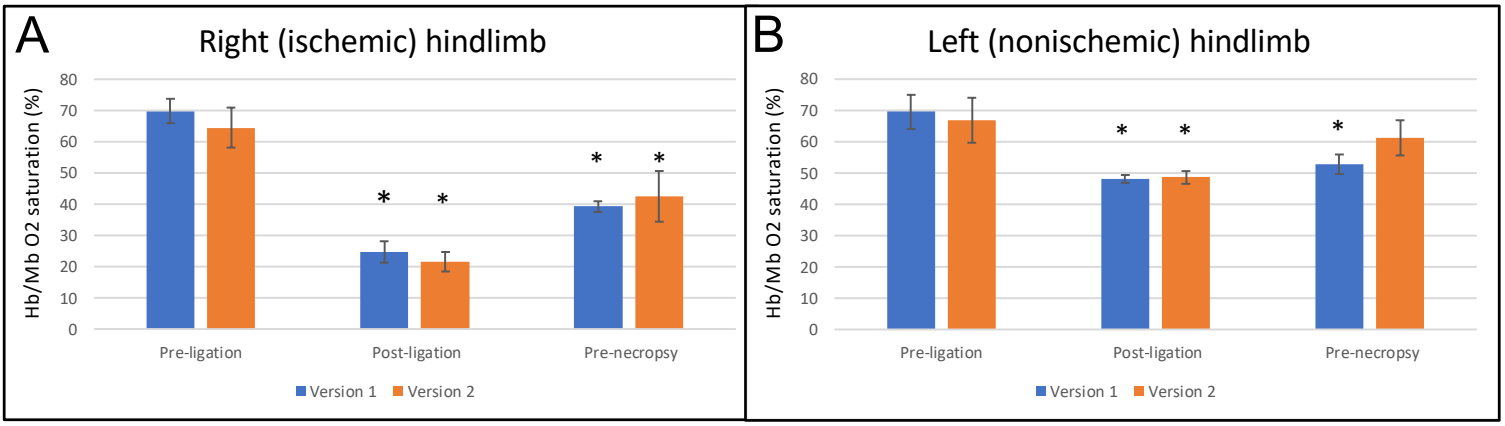

Fig tf07. Muscle hemoglobin/myoglobin oxygen saturation (Moxy), Version 1 *vs.* 2. (A & B) Right and left hindlimb, respectively. Each bar represents mean ± sd of all measurements (raw saturation value) from each subject at each time point; ≥2 measurements were taken at a constant location (medial thigh) at each time point. *p < 0.05 compared to pre-ligation.

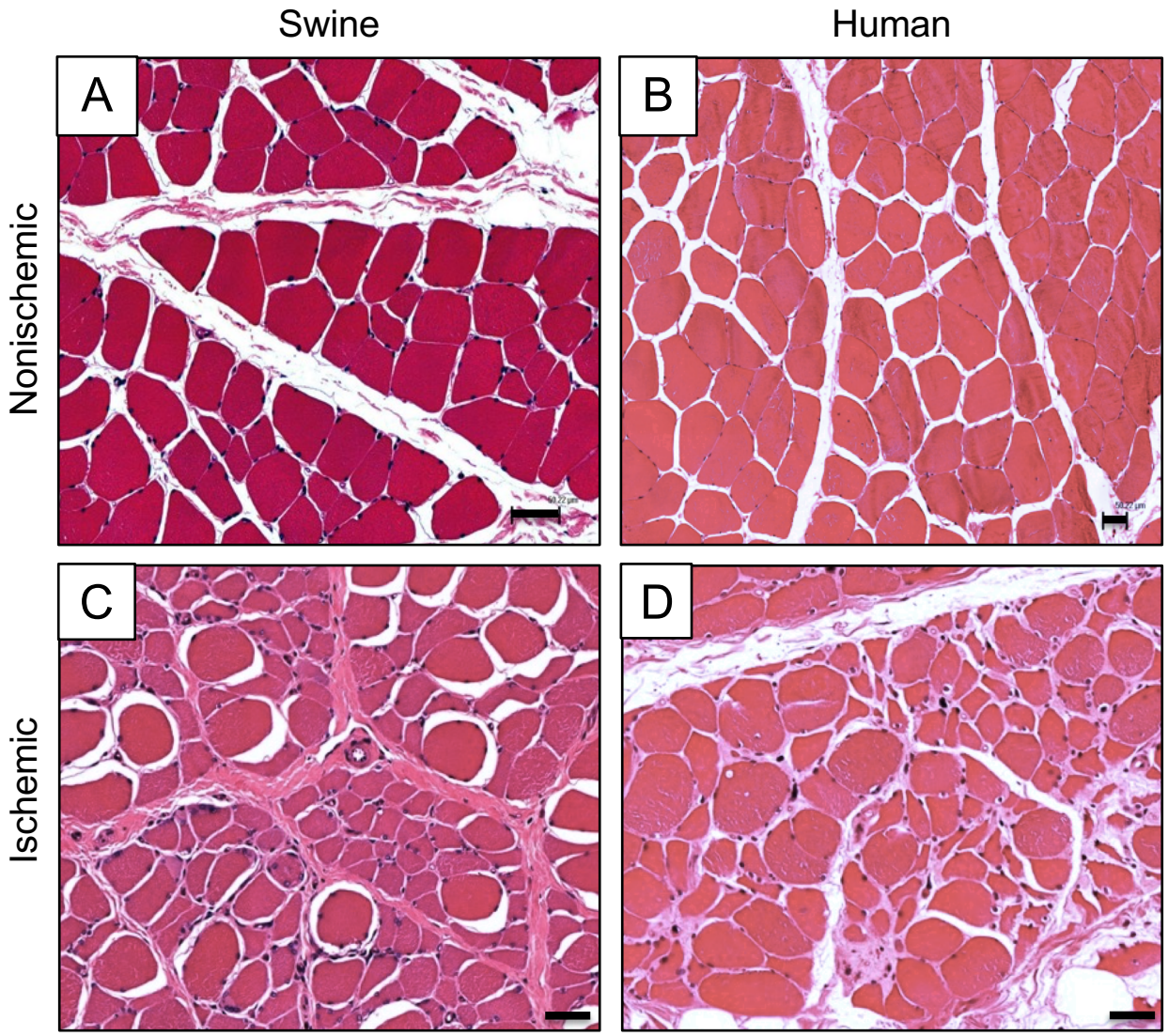

Fig tf08. Ischemic myopathy in porcine vs. human subjects. (A & B) Nonischemic muscle, human vs. porcine, respectively. **(C & D)** Ischemic muscle, human vs. porcine, respectively. Sample from both human and porcine subjects were taken from the medial head of the gastrocnemius muscle. Clinical specimens derived from a separate research protocol that was previously published [insert reference]. Porcine tissue was from the present study (from pre-ligation and pre-necropsy biopsies). H&E; bars = 50 µm.

SUPPLEMENTAL FIGURES

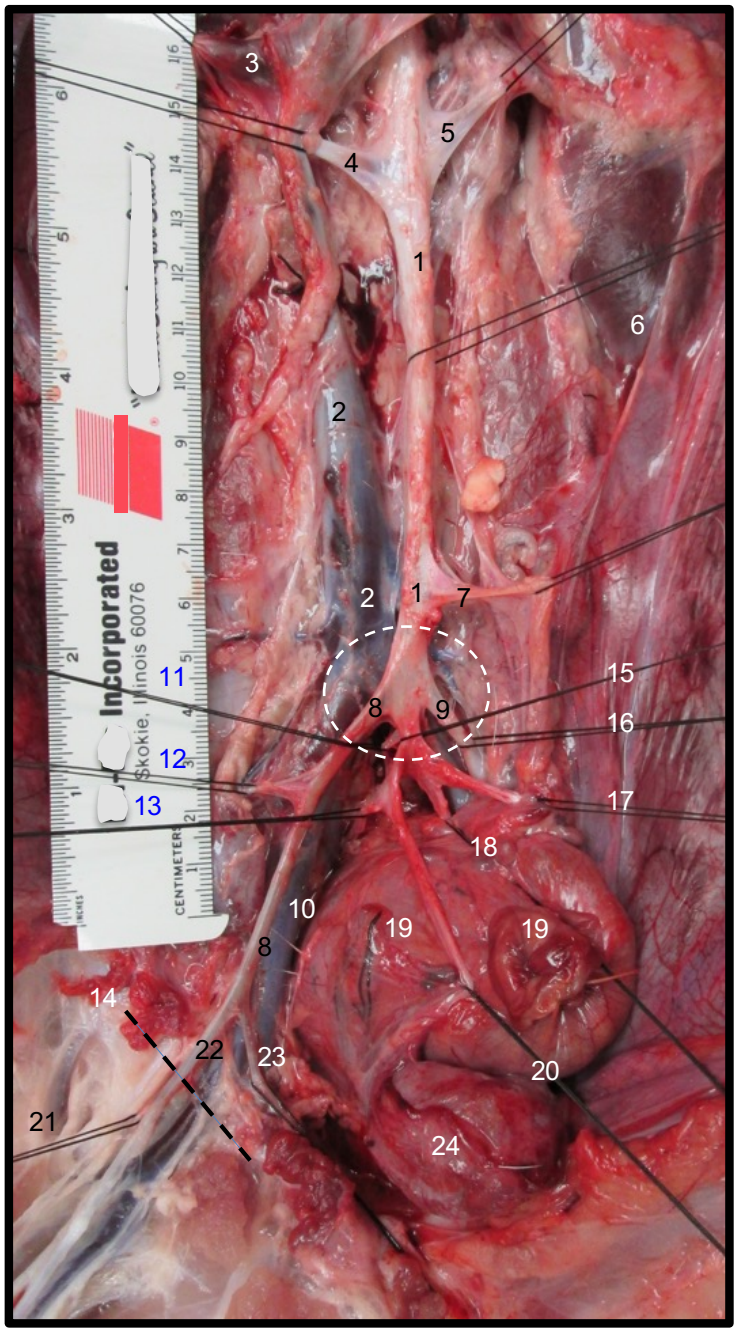

Fig tf09S. Relevant anatomy of the porcine hindlimb.
Nonfixed postmortem dissection of the distal aorta, pelvis, and proximal right hindlimb in the pig. Dashed circle indicates aortic trifurcation.

1. Infrarenal aorta
2. Inferior vena cava
3. Right renal vein
4. Right renal artery
5. Left renal artery
6. Lower pole left kidney
7. Internal mesenteric artery (on silk loop)
8. Right external iliac artery
9. Left external iliac artery
10. Right external iliac vein
11. Middle sacral artery (on silk loop, posterior)
12. Right circumflex iliac artery (on silk loop)
13. Parietal branch of the right internal iliac artery on silk suture
14. Approximate level of inguinal ligament
15. Common internal iliac trunk (on silk loop)
16. Left external iliac artery (on silk loop)
17. Parietal branch of the right internal iliac artery on silk suture
18. Visceral branch of LIIA (on silk loop)
19. Rectal stump
20. Visceral branch of RIIA (on silk loop)
21. Right circumflex femoral artery (on silk loop)
22. Right superficial femoral artery
23. Right profunda femoral artery on silk suture
24. Urinary bladder

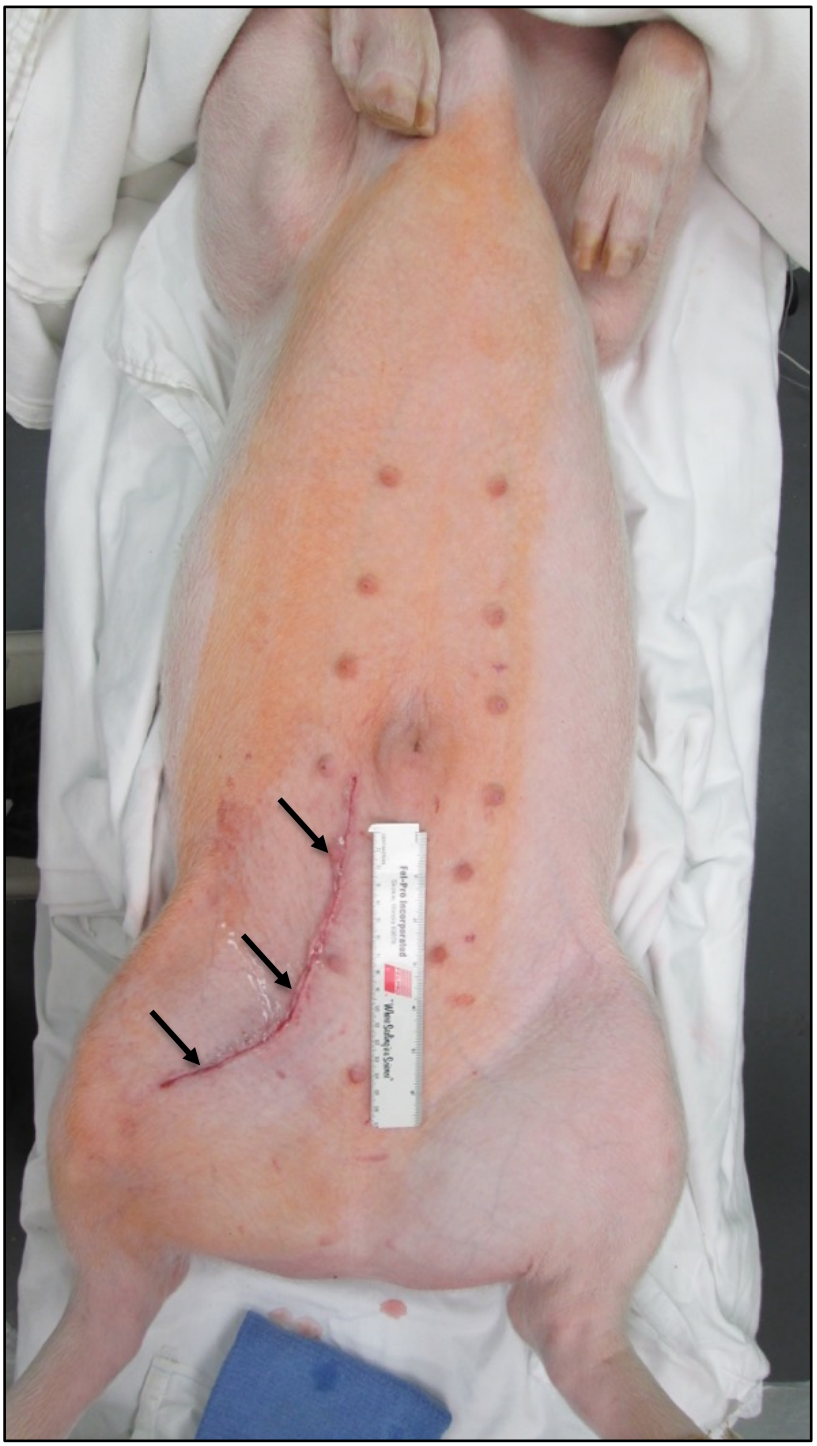

Fig. tf10S. Incision for retroperitoneal dissection. Anesthetized porcine subject is supine, with overhead view of ventral chest, abdomen, and pelvis; cephalad is toward top of image. Freshly closed incision indicated with arrows. Ruler is 15 cm long.

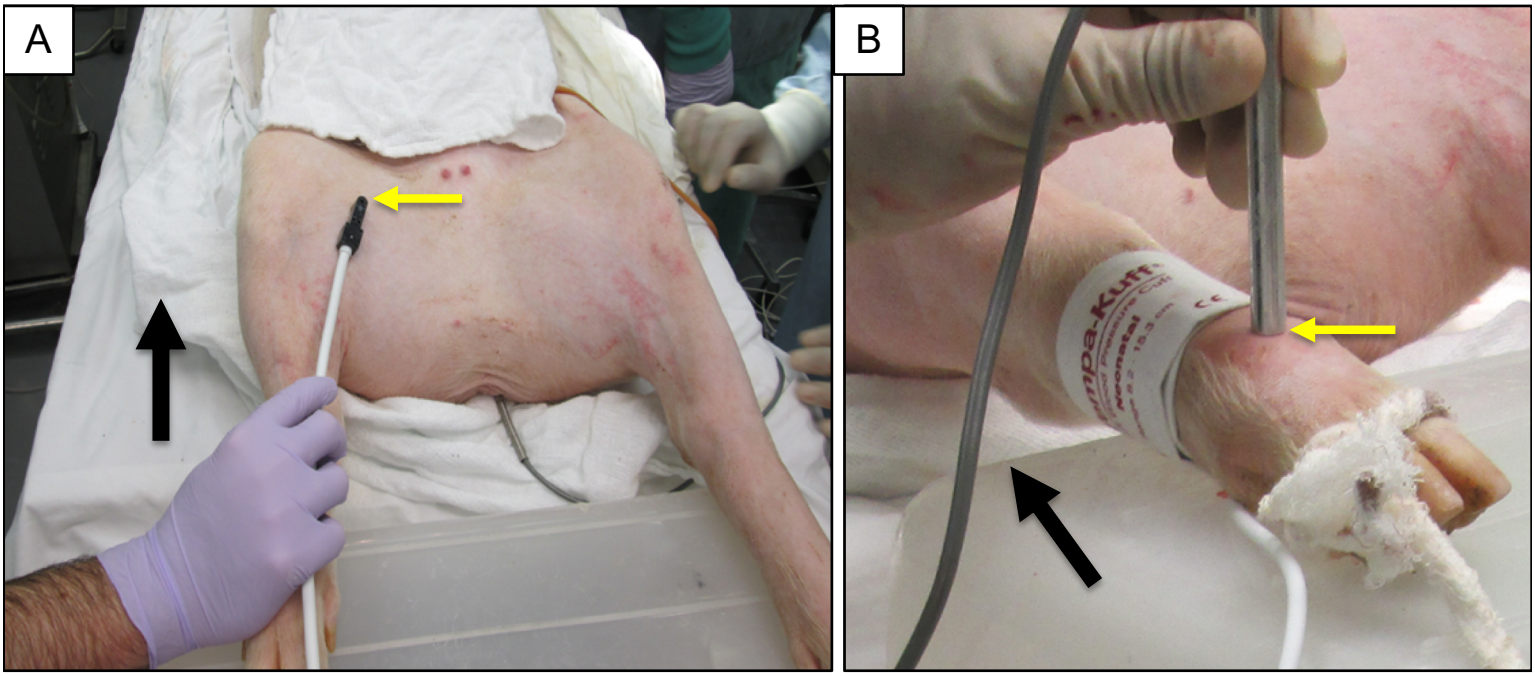

Fig tf11S. Measurements of Moxy and ABI in pigs. **(A)** Transcutaneous measurement of muscle hemoglobin/myoglobin oxygen saturation (Moxy). The Moxy instrument probe (arrow) has been placed over the right medial thigh of the subject. **(B)** Doppler of dorsalis pedis artery (yellow arrow) in the right distal hindlmb, for determination of arterial pressure index. Blood pressure cuff is visible just proximal to doppler probe. Black arrow = cephalad.

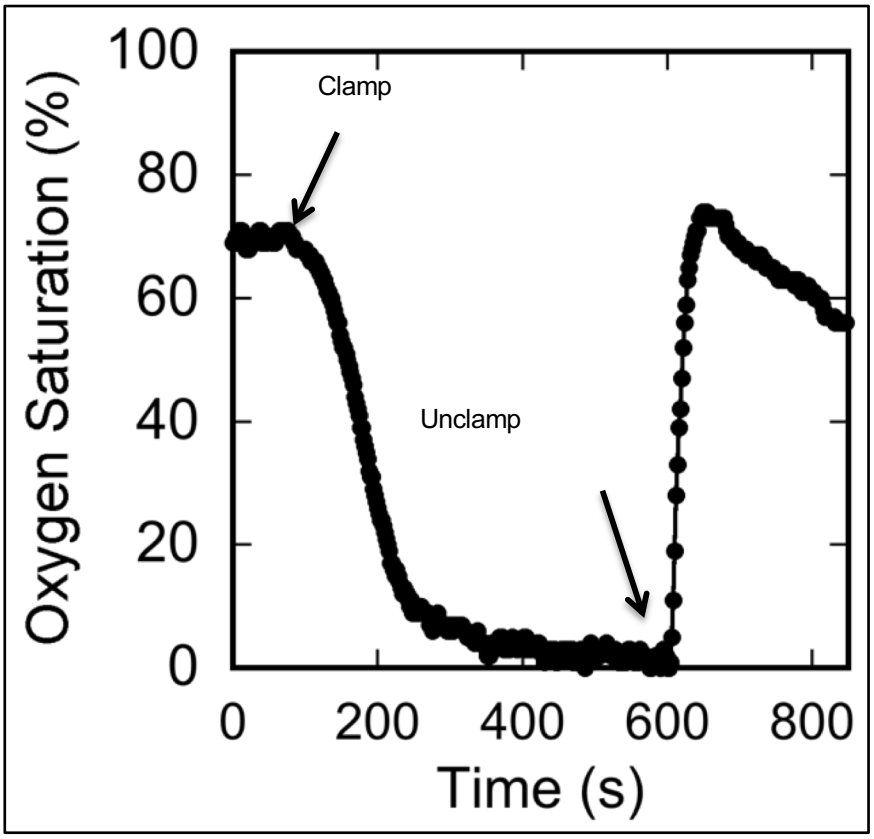

Fig tf12S. Sample tracing of muscle hemoglobin/myoglobin oxygen saturation (Moxy). The plot shows Moxy oximetry readings from of the porcine right medial thigh before, during, and after clamping of the right external iliac artery. There was an abrupt decrease in muscle oxygenation when the femoral artery was clamped and an abrupt increase in oxygenation when the artery was unclamped.

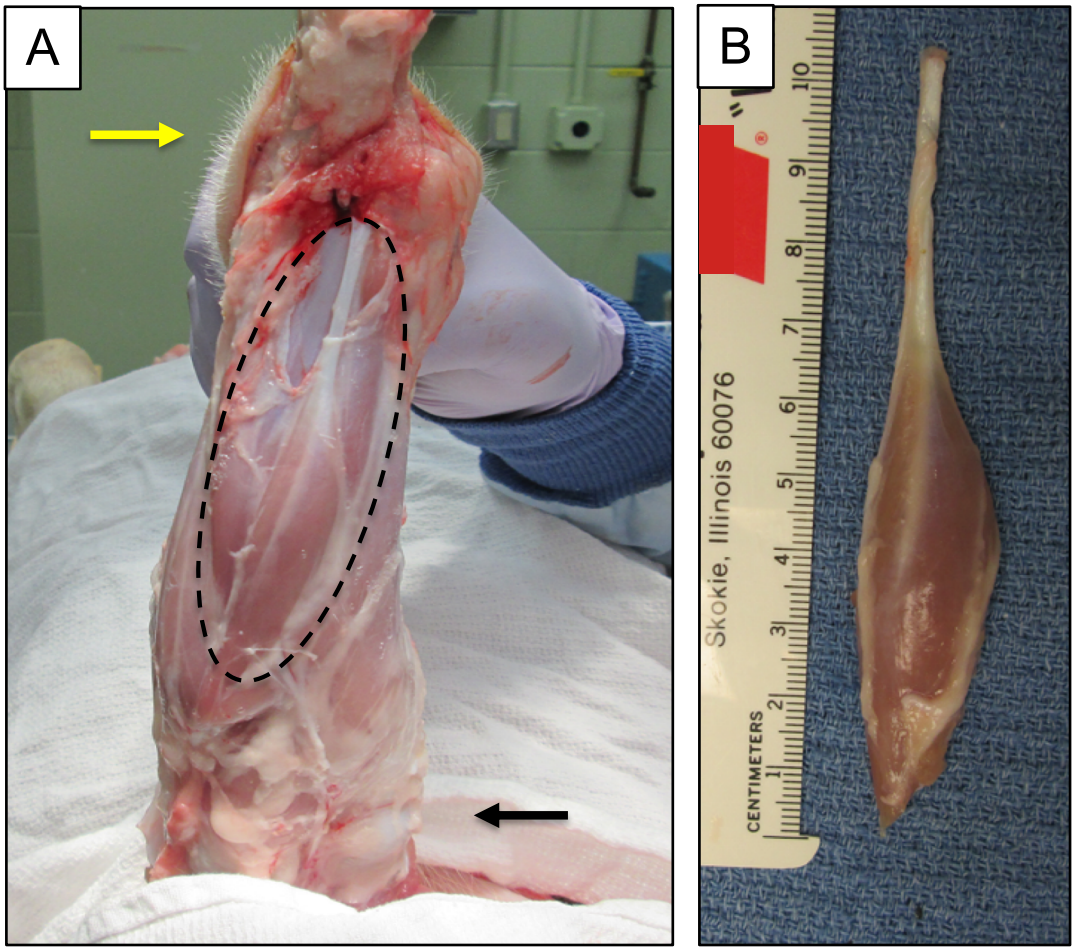

Fig tf13S. Postmortem dissection of porcine hindlimb. (A) Posterior view of right hindlimb, elevated; distal is at top of image, lateral is at left of image; yellow arrow indicates level of ankle joint; black arrow indicates level of knee joint. Gastrocnemius muscles have been dissected away, and are not visible. Dashed oval = plantaris muscle. **(B)** Explanted right plantaris muscle from panel A.